Hysteresis and memory characteristics of GaAs photodetector in a modified IR image converter

H. Y. KURT*, S. ÇETİN, A. YURTSEVEN

Physics Department, Faculty of Sciences, Gazi University, 06500 Ankara, Turkey

The hysteresis and corresponding memory effect were reported in an *IR* image converter from a modified configuration with contact-free photodetector under various operating conditions for the first time to our knowledge. It was considered that the memory effect based on hysteresis plot in the modified configuration was apparently due to charge trapping in the *GaAs* memory detectors. The effect of gas pressure on the *CVC* and the hysteresis curves were studied in detail. It was proven that gas pressure was one of the key parameters affecting the hysteresis width. In addition, the memory effect was found to be sensitive to the illumination intensity on the photodetector.

(Received August 31, 20013; accepted January 22, 2014)

Keywords: *GaAs* photodetector, Gas discharge, Breakdown, hysteresis, Memory effect, *IR* converter

1. Introduction

There are plenty of physical systems which denote hysteresis. Among them, the irreversible processes in ferroelectrics, shape memory behavior in alloys, work hardening processes in mechanical materials, contact angle hysteresis can be mentioned in that sense [1]. Nowadays, the significance of hysteresis has also been discovered in complex systems that shows a large variety of different nonequilibrium phenomena. Among them, memory devices play a crucial role in electronics, receiving interest for more than 20% of the semiconductor market [2]. One of the application areas of memory effect is

optical data storage applications demanding the nonlinear optical materials where the recorded optical data can be stored semipermanently, and

then reversibly erased. One such proposal is based on the multiple read-and-write memory materials, such as the magnetic materials used in magnetic recording, depend on the reversible transformations from one metastable equilibrium state [3]. Furthermore, Sanduloviciu et. al [4] reported that the self-organization concept guarantees the reversibility of the atomic state during energy exchange with the surrounding medium in this manner.

On the other hand, *EL2* centers in semiconductor play an important role for the optical applications [6]. A typical explanation for memory effect is characterized by nonequilibrium phenomena. The mechanism which is the responsible for the memory effect is closely related with the electron capture and emission from *EL2* deep center when the electrode is exposed to forward and reverse feeding voltage [7]. In this case, the charging and discharging of surface state change the conductivity of the semiconductor, which gives a rise to the non-volatile memory effect. The memory effect has not been encountered in the gas discharge gap with two metallic electrodes performed by us and reported in [8]. Therefore; the memory effect is due to the *GaAs* photodetector in the converter [8].

In this manner, *GaAs* is a vital material due to its advanced carrier mobility, extensive band sensitivity (from *VIS* to near *IR*) and large absorption coefficient for optoelectronic applications [6]. Furthermore, *GaAs* is an attractive material due to the high speed response characteristics especially in the range of infrared [9].

This paper focuses on the memory effect based on hysteresis behavior of the ohmic contact-free *GaAs* memory photodetectors in an *IR* image converter cell with *MC* for the first time to our knowledge. In one of our earlier papers, the memory effect was reported in conventional gas discharge cell with a high-resistivity *GaAs* cathode (Fig.1). In this paper, some interesting hysteresis results will be reported in low pressured media in modified *IR* image converter. Some parametrical features of that behaviour will also be defined. We believe that this new structure may find an application in fast sources of the *UV* radiation, which are controlled by the *IR* light [10].

2. Experimental

The experiments are performed in the photodetector system sketched in Fig. 1. This *MC* is the basic element of the *IR*-to-*VIS* image converter having an ultrafast response in the *IR* range of light [6,11]. It is an *IR* image converter with an *MC* which is composed of a photosensitive high resistivity semiconductor layer and two narrow discharge gaps. The *IR* image converter has the small dimension, therefore fast dynamics with the operation of that device can be obtained. Since the wavelength of the used *IR*

radiation is around λ_B = 867 nm, the band gap energy of *GaAs* is found to be around 1.42 eV.

The most important difference between the conventional cell and the present *MC* in Fig. 1 is multiple gas-filled gaps at two sides of the *GaAs* photodetector [12-13]. One of the advantages of this modified configuration, compared with the previous configuration [see Fig. 1)], is that an ohmic contact is not required on the the surface of the photodetector. Since *GaAs* sits at the middle of the gap, the negative effect of contact phenomena is vanished on the *CVC*. Because the production of an ohmic contact with spatially homogeneous feature is hard to maintain for the optimum operation. When a constant dc voltage (V_0 = 200−2000 V) is applied between the electrodes, self-sustained gas discharge takes place in both gaps. The discharge current is managed by a spatially homogeneous *IR* light. The *MC* contains two gas discharge gaps which are sandwiched between two glass plates.

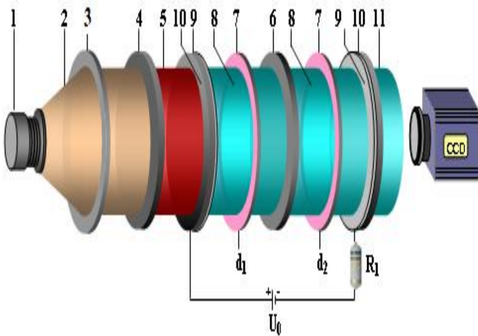

Fig. 1. Schematic diagram of the modified configuration with an ohmic contact-free GaAs photodetector:1-light source; 2-incident light beam; 3- lens; 4-Si filter; 5- IR light beam; 6-GaAs photodetector; 7-mica foil; 8-gas discharge gap; 9-transparent conductive SnO_2 contact; 10-flat glass disc; 11- UV- visible light beam.

For the measurement of the *CVC* in the *MC*, the gas pressure *p* is changed in a sufficiently wide range (28-352 Torr). In this *MC*, the planar photosensitive *GaAs* photodetector is placed between two optically transparent electrodes made by glass, the inner surfaces of them are coated with thin transparent SnO_2 films. The semi-insulating (*SI*) *GaAs* used in the experiments is an *n*-type with high resistivity around $\rho \simeq 10^8$ Ωcm and the sample is oriented in the plane of natural growth of the crystal (i.e. 100). The *GaAs* plate thickness is about 1 mm and the diameter is 40 mm, respectively. The surface of the *GaAs* photodetector is isolated from a flat anode by an insulating mica sheet with a circular aperture at its centre. Diameters of the effective electrode areas change in the range of *D* = 9-15 mm (i.e. gas discharge gap or diameters of the circular through-aperture in the insulator). In the course of the experiments, we use a fixed d_1 as 50 μm and d_2 has varying values between 50 μm and 320 μm. The entire setup is shown in Fig. 2.

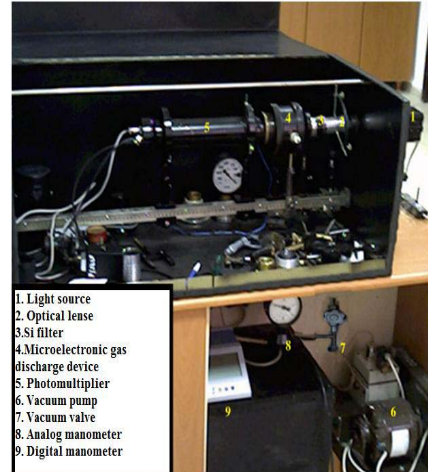

Fig. 2. A photo of IR converter cell. The main part of the system is the discharge cell given by No. 4 (Fig. 1).

3. Results and discussion

We start with Fig.3 for the breakdown event. Fig. 3 shows the breakdown curves for *MC* with various distances *d* between the electrodes and fixed iner diameter *D* of the photodetector. The trend of the breakdown curves in *MC* is similar to the previously given breakdown curves for conventional cells [14-15]. But, left-hand side of the breakdown curves in *MC* is much clearly observed and they increase to higher voltages.

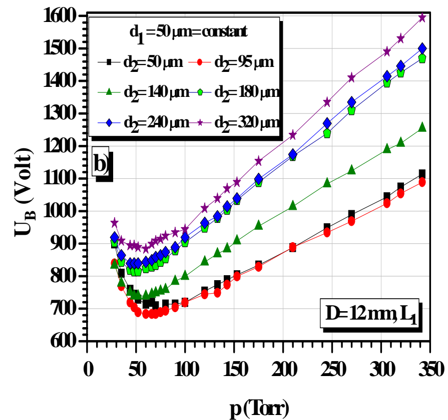

Fig. 3. Experimental breakdown curves for MC with different interelectrode gaps d and weak illumination intensity of light L_1.

The minimum of the Paschen curve is observed around 900 V for *d* = 323 μm, which is larger than the minimum of the same curve of the system that we previously analysed in [14-15]. This situation indicates that the multiple gap systems are much stable compared to the conventional systems. The main difference between the Paschen curves measured in an earlier study and the present one is that the applied voltage is seperated into both narrow gaps. Furthermore, It is shown that the breakdown value U_B of the modified system is much sensitive to the changes in the pressure values [10]. For

this reason, this U_B range is wider than for the usual cell under the same pressure ranges and experimental conditions.

The behaviour of the hysteresis loop is conducted not only by intrinsic properties of material but also by extrinsic factors [16]. In our case, hysteresis curves are recognized by the nonequilibrium process, when the photodetector is exposed to forward and reverse feeding voltage [17]. Fig. 4a shows the current-voltage hysteresis loops of *GaAs* memory detectors in the counter-clockwise direction. Routes to hysteresis are clearly shown in Fig.4a. The recorded hysteresis curves demonstrate that loop is unstable over the sequential sweeps. It is proposed that an unstable electron trapping process can explain the working principle of this memory effect and such hysteresis. The arrows indicate the directions of the applied voltage.

In order to explain the formation mechanism of the intrinsic current oscillations, we analysed time dependence of the current oscillations inside the *NDR* region in Fig. 4b. Time-dependent current oscillations at different feeding voltages of the forward bias sweep are shown in Fig. 4b in the *MC*. We showed that interelectrode distance *d* played an important role in order to classify the dynamics of the system in [14]. Similarly, we observed the *N* shape (*NDR*) oscillatory behaviour in currents beyond a critical *d* (50 μm), which is resulted by an oscillatory bifurcation from a stationary state.

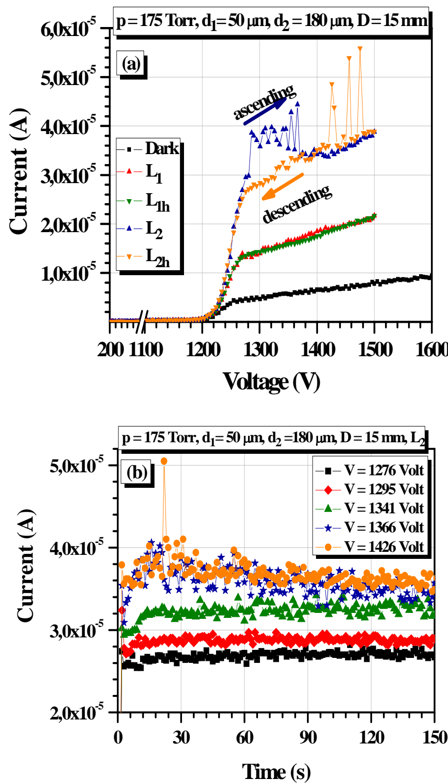

Fig. 4(a). CVCs with N-shaped and hysteresis behaviour for MC with GaAs photodetector; curves refer to forward and reverse directions of U_0, when the GaAs photodetector is exposed to L_2 and L_1 illumination intensities and in darkness, respectively. (b) The time dependence of current oscillations (i.e., different region of CVCs of Fig. 3a) in the MC.

To determine the oscillatory and *N*-shaped of current voltage behaviour in *SI GaAs*, *TEE* is considered. In fact; an electric-field enhances the transfer of electrons from low-energy and high mobility to a higher-energy and lower mobility one. In that case, the current oscillations are originated by high electric field region that moves from cathode to anode [18]. On the other hand, the memory effect is sensitive to the illumination intensity on the photodetector as seen in (Fig. 5). At this point, it is also important to remind that photoeffect plays an important role to produce such kind of memory effect [19]. Experimental results show that trap levels exist on the *GaAs* surface, and these levels have a different influence on the current under forward and reverse of feeding voltage directions.

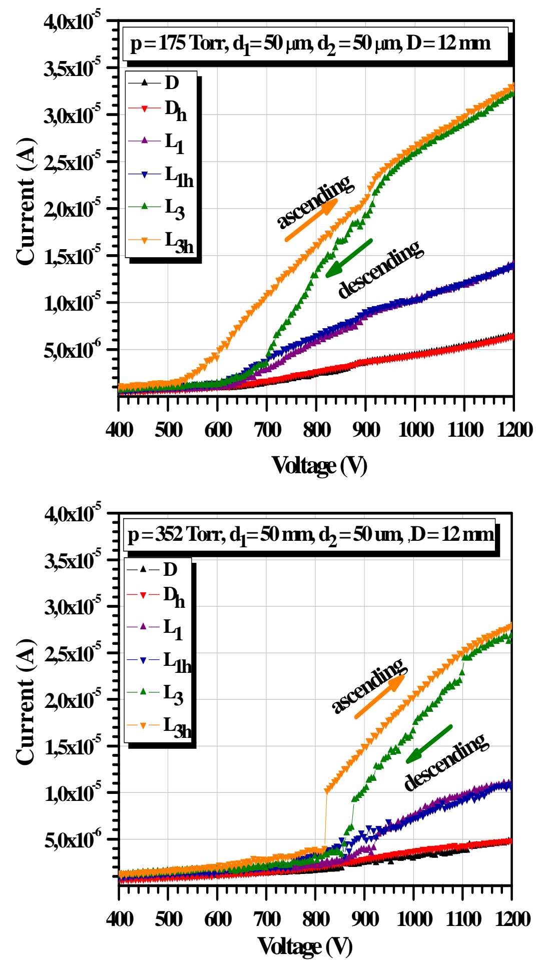

Fig. 5. Illumination effect on the hysteresis behaviour in the MC for p =175 and 352 Torr.

These results indicate that surface charge has an considerable influence on the carrier transport, too. It is a well known process about the surface state of *GaAs* which captures electrons [20]. The illumination procedures described above can clearly produce trapped charge changes on the surface of photodetector that could result in

the hysteresis existence. The resistivity of the *GaAs* photodetector diminish in a monotonic manner when the intensity of the irradiation is increased. According to the literature, this effect is known to arise so-called *EL2* centres in *GaAs.* (refer to [18])

Other two key parameters which affect the shape of the memory curve are the photodetector type and cell pressure. For this reason, the hysteresis measurements are repeated by different pressure. Fig. 6 represents the currents versus pressure in the forward and backward bias sweep. These results differ from Fig. 4a. The hysteresis loop is stable over multiple successive sweeps unlike the hysteresis loop in Fig. 4 for small electrode separation (d=65μm) as expected. The experimental observations show that the current stability for the case of small gap spacing becomes higher than that for the case with larger gap spacing. Hysteresis width changes as function of pressure. This reality enforces us to believe that the hysteresis loop is caused in the lower voltage range due to the traps. A pronounced hysteresis can be observed for p = 90 Torr and 175 Torr, shown in Fig. 6. From the Fig.6, it is clear that the *GaAs* photodetector shows very poor memory behavior for 348 Torr compared to the memory hysteresis obtained from 90 Torr and 175 Torr.

Finally, we have observed a significant influence of the pressure on the magnitude of the (*CVC*) memory window as shown in Figs. 6(a-c). As the pressure is increased from 90 to 348 Torr, the *C–V* memory hysteresis magnitude changed and charge storage efficiency improved. The memory window (The *C–V* hysteresis window width ΔV) is about 63 V at p = 90 Torr; 86 Volt at p = 175 Torr and 41 Volt at p = 348 Torr. It should be noted that the observed hysteresis is characterized by its width ΔV. The above experimental observations prove that the filled gas pressures affects the hysteresis width effectively. At higher pressure rates, the hysteresis effect decreases due to the lower hysteresis width.

Further, the memory window which was observed in this study is encountered for substantially smaller interlectrode distance d, when we compare the findings in a previous structure [22]. In the present study, it has been observed that the lower pressure range and small distance assist to achieve good memory window. Since the semiconductor is positioned at the middle of the cell there is no need to use of *Au* ohmic contact [21].

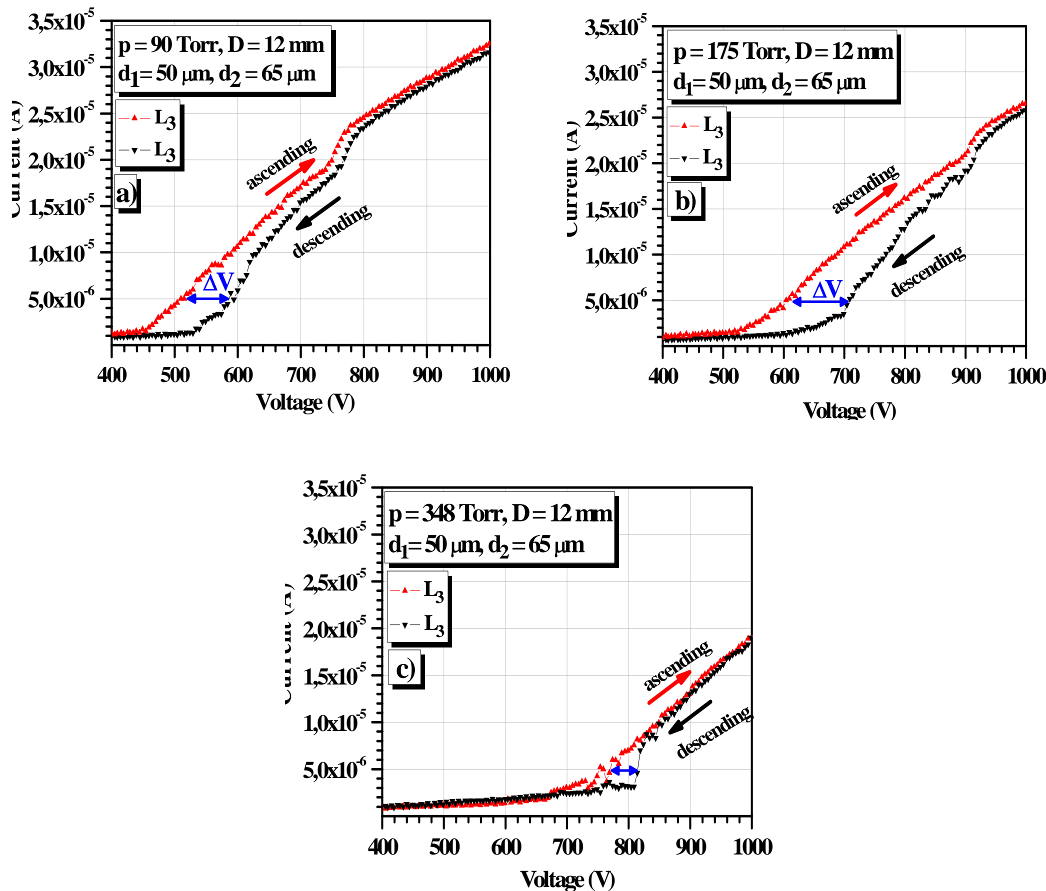

Fig. 6(a-c). Pressure dependence of the hysteresis behaviour for MC with GaAs photodetector under forward increase and reverse decrease of feeding voltage on MC when the GaAs photodetector exposed to strong illumination intensity L_3. System parameters d = 65μm, D = 12 mm.

We think that this situation also contributes to the hysteresis behaviour at low pressure regime. In fact, the exclusion of the ohmic contact decreases the surface charge state of the *GaAs* cathode and yields to much lower current values relative to the previous findings [9]. The commands of Gurevich et.al. [23] are also in that direction. According to him, surface charge affects the physical processes with an ohmic electrode because of the conduction properties of semiconductors, thereby the surface charge is deposited and stored on the surface by reducing the external electric field giving a reduction to the discharge current. However, according to our results the filled gas pressure also

plays an important role at current values of discharge.

The interelectrode distance dependence of hysteresis is shown in Fig. 7.

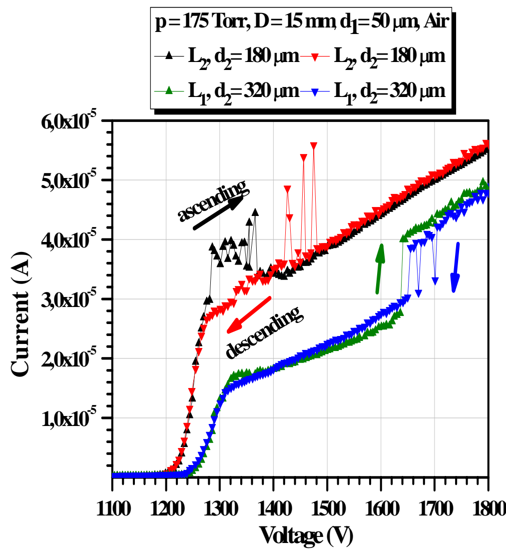

Fig. 7. Hysteresis loops of various interelectrode distances in the MC.

When the interelectrode distance *d* of the *MC* is small, we observed a good memory window in contrast to the previous system with single gap and ohmic contact. It is likely that this change is due to the fact that charge trapped centers through the *GaAs* photodetector, becomes significant when the thickness is decreased to a certain value (i.e. $d \leq 320$ μm)

Thus, we observe a hysteresis in the current range of 3×10^{-5} - 4×10^{-5} A. In addition, one can observe the amplitude of current oscillations changes with regard to the interelectrode distance. In order to determine the memory effect of the *GaAs* detector, we have realized a series of special experiments with that new structure. The memory effect is shown in Fig. 8a where the post-breakdown current values at individual voltage cases for different operation times were considered. In our case the initial measurement time (Start), 24 hours and 48 hours after the initial measurement times were adjusted as different operation times at the same pressure and other system parameters. The memory behaviour produces three different curves for different time intervals. That steems from the charging/discharging of surface states of the semiconductor. The active charges are accumulated on the *EL2* defects being in semiconductor surface (middle of the gap). While the current at the initial measuremet is around 1×10^{-5} A, it increases to $2,5\times10^{-5}$ A and $3,2\times10^{-5}$A after each 24 hours. That proves the memory behaviour of the *GaAs* photodetector.

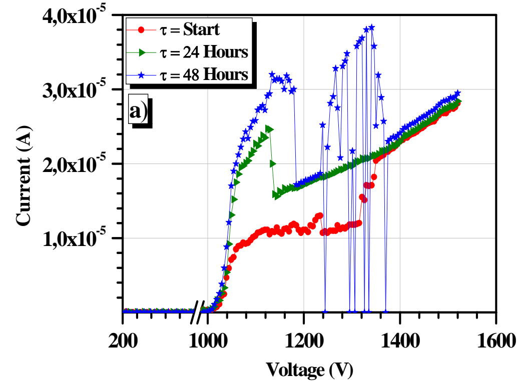

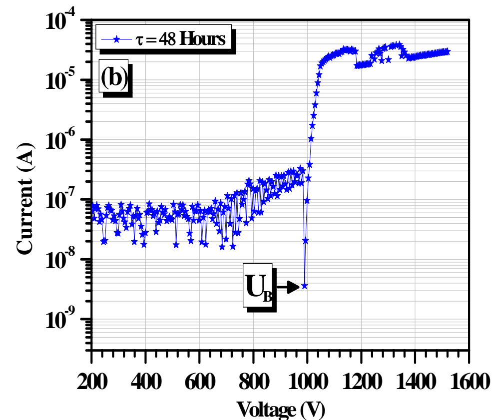

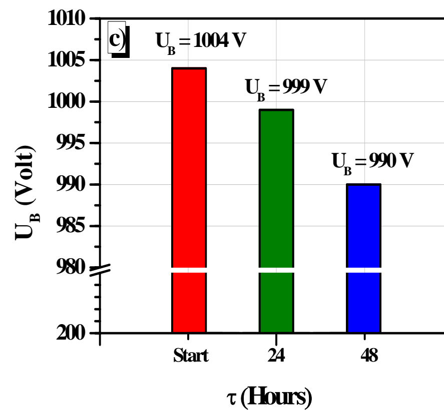

Fig. 8. (a) CVCs for modified discharge cell with the GaAs memory detector measured on different intervals; start, 24 and 48 h, respectively. (b) Logarithmic scale of CVC curve for 48 h. (c) Time dependence of breakdown voltage U_B (start, 24 and 48 h). System parameters, p = 120 Torr, d = 320μm, D = 12 mm.

By realizing detailed measurements on the breakdown stages the following values are found: The current of 3,5 × 10^{-9} A is recorded at breakdown U_B = 990V (see Fig. 8(b) in the logarithmic scale). After this threshould voltage value, current starts to increase. When a high enough voltage (U_0) is applied across the discharge gap, the ionization of gas is initiated. In order to show the memory effect as function of breakdown voltage U_B, Fig. 8c is depicted at 120 Torr. U_B decreases smoothly for increasing operation time after the successive discharges. From these results, we conclude that the U_B values are reduced from 1004V to 990V because of the accumulation of charges on *GaAs* which causes lower U_B values after each successive operation.

From our experimental result we can judge that a larger memory effect have influence upon the results in a lower U_B value. The experimental results are in good agreement with other independent authors studying in different systems. Since the *GaAs* photodetector does not require any ohmic contact, the disadvantages of the contact has been eliminated, thus a much convenient manufacturing of the image convertor can be realized.

4. Conclusion

The hysteresis and corresponding memory behaviors associated with the accumulated surface charges and filled gas pressure were defined in a modified *IR* image convertor. It has been observed that the width of the hysteresis is inverse-proportional to pressure and interelectrode distance in the *MC*. In addition, the external light intensity affects the hysteresis curve and increases the window width. The post-breakdown currents have lower values relative to the earlier *IR* image convertor (i.e. usual cell). Memory effect in the *IR* convertor decreases the breakdown voltage at lower currents. The charge trapping also plays an important role to form the memory behavior. As a conclusion, in compare with the usual converter cells, the present hysteresis character occurs at lower voltages, interelectrode distance and pressures. For future work, the thickness of the *GaAs* photocathode in *MC* can be analysed further for the improvement of the performance of the *IR* image converter.

Acknowledgements

This work was supported by Gazi University BAP research projects **05/2012-47**, **05/2012-72**.

References

[1] O. Hovorka, A Thesis Submitted to the Faculty Of Drexel University by in partial fullment of the requirements for the degree of Doctor of Philosophy August 2007.

[2] S. Paul, A. Kanwal, M. Chhowalla, Nanotechnology.**17**, 145 (2006).

[3] D. D. Nolte, J. Appl. Phys. **79**, 7514 (1996).

[4] M. Sanduloviciu, D. G. Dimitriu, L. M. Ivan, M. Aflori, C. Furtuna, S. Popescu, E. Loznean, J. Optoelectron. Adv. Mater.. **7**, 845 (2005).

[5] D. L. Budnitskii, O. B. Koretskava, O. P. Tolbanov, A. V. Tyazhev, Russian Physics Journal.**53**, 44 (2010).

[6] B. G. Salamov, H. Y. Kurt, J. Phys. D: Appl. Phys. **38**, 682 (2005).

[7] F. S. Gabibov, E. M. Zobov, Inorganic materials. **49**, 810 (2013).

[8] B. G. Salamov, N. N. Lebedeva, H. Y. Kurt, V. I. Orbukh, E. Yu. Bobrova, J. Phys. D: Appl. Phys. **39**, 2732 (2006).

[9] Y. Sadiq, H. (Yucel) Kurt, A. O. Albarzanji, S. D. Alekperov, B. G. Salamov, Solid-State Electronics. **53**, 1009 (2009).

[10] H. Kurt, S. Cetin, B. G Salamov, IEEE Transactions on Plasma Science. **39**, 1086 (2011).

[11] K. Aktas, S. Acar, B. G. Salamov, Plasma Sources Sci. Technol. **20**, 045010 (2011).

[12] Y. Sadıq, K. Aktas, S. Acar, B. G. Salamov, Superlattices and Microstructures. **47**, 648 (2010).

[13] H. Y. Kurt, A. Inaloz, B. G. Salamov, Optoelectron. Adv. Mater. **4**, 205 (2010).

[14] L. Gurevich, S. Kittel, R. Hergenroder, Yu. A. Astrov, L. M. Portsel, A. N. Lodygin, V. A. Tolmachev, A. V. Ankudinov, J. Phys. D: Appl. Phys. **43**, 275302 (2010).

[15] H. Y. Kurt, Y. Sadiq, B. G. Salamov, Physica Status Solidi A-Applications and Materials Science. **205**, 321 (2008).

[16] A. Inaloz, H. Y. Kurt, E. Koc, B. G. Salamov, Physica Status Solidi A-Applications and Materials Science. **206**, 2559 (2009).

[17] J.-H. Park, S. H. Yoon, D. Shen, S.-Y. Choe, Y. S. Yoon, M. Park, D.-J. Kim, J Mater Sci: Mater Electron. **20**, 366 (2009).

[18] E. H. Lemus, E. Orgaz, Rev. Méx. Fis. **48**, 38 (2002).

[19] S. Nguyen, A. Stesmans, V. V. Afanasev, Microelectronic Engineering. **109**, 294 (2013).

[20] M. M. Pejovic, G. S. Ristic, Z. Lj Petrovic, J. Phys. D: Appl. Phys. **32**, 1489 (1999).

[21] S. Stauss, H. Muneoka, N. Ebato, F. Oshima, D. Z. Pai, K. Terashima, Plasma Sources Sci. Technol. **22**, 025021 (2013).

[22] Y. Sadiq, H. (Yucel) Kurt, B. G. Salamov, J. Phys. D: Appl. Phys. **41**, 225204 (2008).

[23] C. Meyer, J. Franzke, E. L. Gurevich, J. Phys. D: Appl. Phys. **45**, 355205 (2012).

*Corresponding author: hkurt@gazi.edu.tr